Structurally and functionally unique complexins at retinal ribbon synapses

Kerstin Reim,[1] Heike Wegmeyer,[1] Johann Helmut Brandstätter,[2,7] Mingshan Xue,[3,4] Christian Rosenmund,[3,4] Thomas Dresbach,[5] Kay Hofmann,[6] and Nils Brose[1]

[1]Department of Molecular Neurobiology, Max-Planck-Institute for Experimental Medicine, D-37075 Göttingen, Germany
[2]Department of Neuroanatomy, Max-Planck-Institute for Brain Research, D-60528 Frankfurt/Main, Germany
[3]Department of Neuroscience and [4]Department of Molecular and Human Genetics Baylor College of Medicine, Houston, TX 77030
[5]Institute for Anatomy and Cell Biology, Ruprecht-Karls-University Heidelberg, D-69120 Heidelberg, Germany
[6]Bioinformatics Group, MEMOREC Biotech GmbH, D-50829 Köln, Germany
[7]Institute for Zoology, University of Erlangen-Nürnberg, D-91058 Erlangen, Germany

Ribbon synapses in retinal sensory neurons maintain large pools of readily releasable synaptic vesicles. This allows them to release several hundreds of vesicles per second at every presynaptic release site. The molecular components that cause this high transmitter release efficiency of ribbon synapses are unknown. In the present study, we identified and characterized two novel vertebrate complexins (CPXs), CPXs III and IV, that are the only CPX isoforms present in retinal ribbon synapses. CPXs III and IV are COOH-terminally farnesylated, and, like CPXs I and II, bind to SNAP receptor complexes. CPXs III and IV can functionally replace CPXs I and II, and their COOH-terminal farnesylation regulates their synaptic targeting and modulatory function in transmitter release. The novel CPXs III and IV may contribute to the unique release efficacy of retinal sensory neurons.

Introduction

Sensory neurons in the retina use graded potentials to transmit sensory information. By this mechanism, they are able to continuously adjust their synaptic output to changing inputs and thus optimize information transfer (Parsons and Sterling, 2003). As the synaptic output of sensory neurons is initiated by exocytotic neurotransmitter release from synaptic vesicles, its continuous adjustment over a physiologically relevant range requires that large numbers of synaptic vesicles fuse with the plasma membrane at very high rates (Parsons and Sterling, 2003). In the retina, the photoreceptor cells and their second-order neurons, the bipolar cells, can release several thousands of synaptic vesicles per second. In terms of individual release sites, this represents an exocytosis rate of several hundred vesicles per second (Heidelberger et al., 1994; Parsons et al., 1994; Rieke and Schwartz, 1996; von Gersdorff et al., 1996). This high rate of release exceeds that of conventional synapses by a factor of 30 (Stevens and Tsujimoto, 1995), and is made possible because sensory neurons have large numbers of primed and readily releasable vesicles that can be exocytosed via a rapid release mechanism.

A main factor contributing to the extreme exocytotic performance of sensory neurons is the organization of their release sites, or active zones. Conventional active zones at glutamatergic synapses in the mammalian central nervous system are characterized by a flat, electron-dense structure that is associated with the presynaptic plasma membrane and from which fuzzy electron-dense projections emanate into the surrounding cloud of synaptic vesicles. In contrast, presynaptic active zones in retinal photoreceptors and bipolar cells, and also in inner ear sensory neurons and in neurons within the pineal gland, contain a specialized plate-like organelle, the ribbon. Each ribbon is anchored to the presynaptic plasma membrane in close vicinity to voltage-gated Ca^{2+} channel clusters, and tethers some 100 synaptic vesicles via short filamentous connections. It is thought that the vesicles tethered to the ribbon are readily releasable and that they release their transmitter content by compound fusion (Parsons and Sterling, 2003). Anchored ribbons are essential for normal photoreceptor ribbon synaptic transmission (Dick et al., 2003).

Unique molecular constituents are likely to be responsible for the extraordinary morphological and functional characteristics

K. Reim, H. Wegmeyer, J.H. Brandstätter, and M. Xue contributed equally to this work.

Correspondence to Nils Brose: brose@em.mpg.de

Abbreviations used in this paper: CPX, complexin; DIV, d in vitro; DKO, double KO; GCL, ganglion cell layer; INL, inner nuclear layer; IPL, inner plexiform layer; KO, knockout; OPL, outer plexiform layer; PNA, peanut agglutinin; RRP, readily releasable vesicle pool; SNAP-25, synaptosomal-associated protein of 25 kD; wt, wild-type.

The online version of this article contains supplemental material.

Supplemental material can be found at:
http://doi.org/10.1083/jcb.200502115

The Journal of Cell Biology, Vol. 169, No. 4, May 23, 2005 669–680
http://www.jcb.org/cgi/doi/10.1083/jcb.200502115

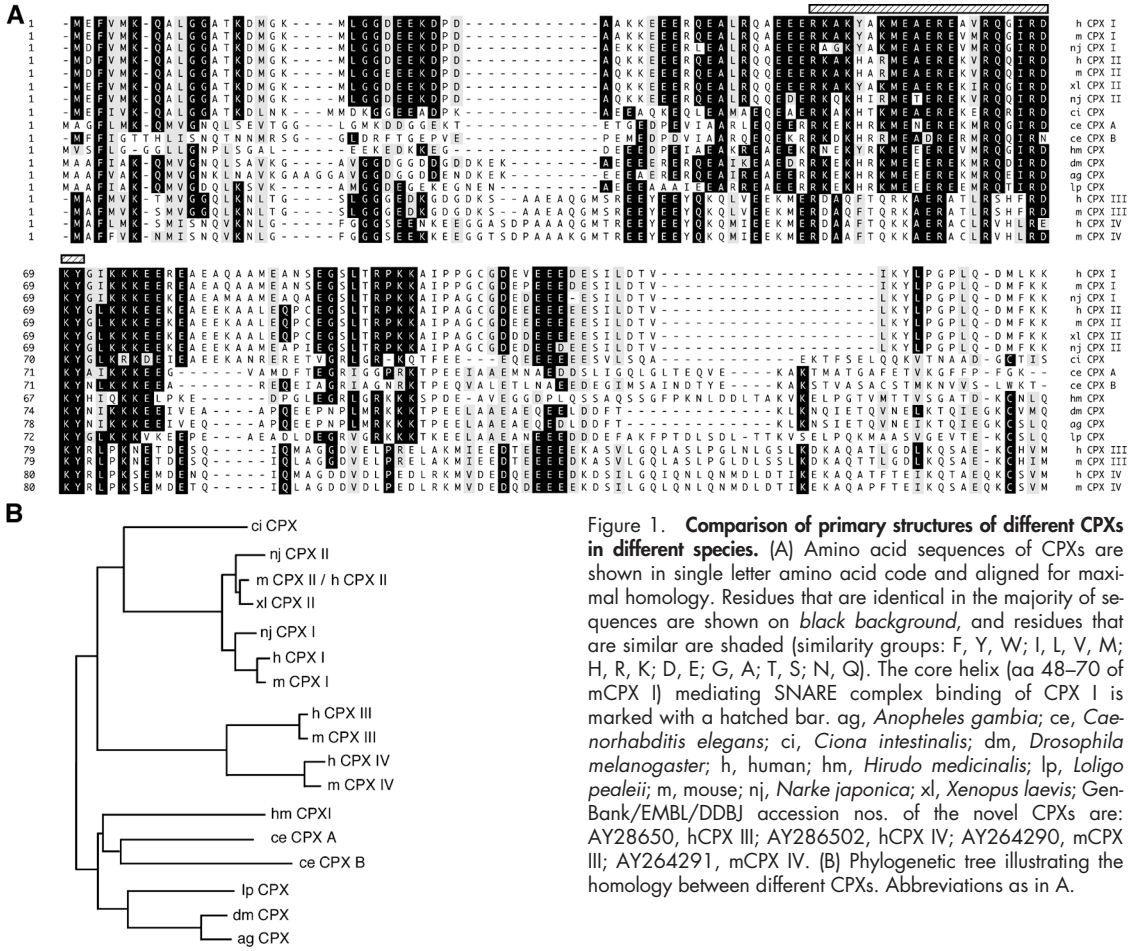

Figure 1. **Comparison of primary structures of different CPXs in different species.** (A) Amino acid sequences of CPXs are shown in single letter amino acid code and aligned for maximal homology. Residues that are identical in the majority of sequences are shown on *black background*, and residues that are similar are shaded (similarity groups: F, Y, W; I, L, V, M; H, R, K; D, E; G, A; T, S; N, Q). The core helix (aa 48–70 of mCPX I) mediating SNARE complex binding of CPX I is marked with a hatched bar. ag, *Anopheles gambia*; ce, *Caenorhabditis elegans*; ci, *Ciona intestinalis*; dm, *Drosophila melanogaster*; h, human; hm, *Hirudo medicinalis*; lp, *Loligo pealeii*; m, mouse; nj, *Narke japonica*; xl, *Xenopus laevis*; GenBank/EMBL/DDBJ accession nos. of the novel CPXs are: AY28650, hCPX III; AY286502, hCPX IV; AY264290, mCPX III; AY264291, mCPX IV. (B) Phylogenetic tree illustrating the homology between different CPXs. Abbreviations as in A.

of retinal ribbon synapses. However, only very few ribbon synapse specific proteins have been identified. One such protein is RIBEYE, a structural component of ribbons with unknown function (Schmitz et al., 2000). In addition, Ca^{2+} channels (L-type at ribbon synapses and N-, P/Q-, or R-type at conventional synapses; Heidelberger and Matthews, 1992; Nachman-Clewner et al., 1999; Morgans, 2001), syntaxins (syntaxin 3 at ribbon synapses and syntaxin 1 at conventional synapses; Morgans et al., 1996), and synapsins (synapsins I and II are absent from ribbon synapses; Mandell et al., 1990) are differentially distributed between ribbon synapses and conventional synapses.

Apart from above examples, ribbon synapses contain largely the same proteins as conventional synapses. This also applies to the SNARE proteins synaptosomal-associated protein of 25 kD (SNAP-25) and VAMP/synaptobrevin 2, which together with syntaxins 1, 2, or 3 mediate the actual synaptic vesicle fusion reaction with the plasma membrane (Jahn et al., 2003). SNARE complex function at synapses is regulated by a number of interacting proteins which are responsible for the characteristic spatial restriction, speed, and Ca^{2+} dependence of neurotransmitter release. Among these SNARE-regulating proteins are complexin (CPX) I and CPX II, which regulate a late step in the release process, most likely by stabilizing SNARE complexes and thus maintaining synaptic vesicles in a highly release competent state (Reim et al., 2001; Chen et al., 2002).

We show here that the essential SNARE regulators CPXs I and II are not present at retinal ribbon synapses. Instead, ribbon synapses in the retina contain two members of a novel mammalian CPX subfamily, CPX III and CPX IV, which exhibit unusual structural and functional characteristics.

Results

Structure and conservation of CPX isoforms

Using protein profile searches, we identified two genes in current genomic databases (CELERA) which encode two novel CPXs, CPX III and CPX IV. We assembled the complete human CPXs III and IV coding sequences from genomic sequence data (CELERA: GA_x5YUV32W5LP for CPX III and GA_x5YUV32VUQQ for CPX IV), then designed PCR primers, and amplified the full-length human CPXs III and IV cDNAs from brain cDNA. Based on the human sequence, the cDNAs of murine CPXs III and IV were PCR amplified from mouse brain cDNA. The cloned cDNA sequences were almost identical to the sequences deduced from genomic data and were used for subsequent comparative sequence analyses (Fig. 1 A). Database searches revealed no evidence for additional CPX genes in the human genome. Human and murine CPXs III and IV cDNA sequences were deposited in GenBank (GenBank/

EMBL/DDBJ accession nos. AY286501 [hCPX III], AY286502 [hCPX IV], AY264290 [mCPX III], and AY264291 [mCPX IV]).

Alignment of murine amino acid sequences revealed that the two new members of the CPX family are highly homologous (58% identity) to each other, but show only limited homology with CPXs I and II (24–28% identity; Fig. 1 B). Like CPXs I and II, CPXs III and IV are small, highly charged molecules, containing 158 residues (17.6 kD) and 160 residues (18.3 kD), respectively. In contrast to CPXs I and II, CPXs III and IV contain a CAAX-box motif at their COOH termini (Fig. 1 A) which represents a consensus sequence for posttranslational prenylation (Zhang and Casey, 1996). Comparison of mouse and human CPX sequences showed that the respective CPXs III and IV orthologues are very similar to each other, with over 91% identity at the amino acid level. The corresponding sequence identity between murine and human CPXs I and II orthologues is 97 and 100%, respectively. Several invertebrate species express CPXs that contain CAAX-boxes but are otherwise more similar to murine and human CPXs I and II (Fig. 1, A and B).

Expression pattern of CPX mRNAs

To analyze the expression pattern of CPXs III and IV mRNAs, we hybridized blots loaded with poly(A)$^+$ RNA from rat heart, brain, spleen, lung, liver, skeletal muscle, kidney, and testis with full-length mouse CPXs III and IV cDNA probes. No signals were detected on these blots.

We next searched EST databases for CPX sequences and their tissue origin. All identified mCPX IV ESTs were derived from eye or retina. Likewise, mCPX III ESTs were mostly derived from eye or retina, but also from whole brain or visual cortex. To test if the new CPXs III and IV are preferentially expressed in retina, we compared the expression pattern of mRNAs of all known CPX isoforms in rat brain and retina by hybridizing blots loaded with poly(A)$^+$ RNA from whole rat brain and rat retina at high stringency using full-length rat CPX I (GenBank/EMBL/DDBJ accession no. U35098), rat CPX II (GenBank/EMBL/DDBJ accession no. U35099), mouse CPX III, and mouse CPX IV cDNA probes. CPXs I and II mRNAs were found in brain and retina whereas CPXs III and IV transcripts were only detectable in retina (Fig. 2 A).

As mentioned above, the CPXs III and IV cDNAs were amplified from brain cDNA and the mouse EST search showed that there must be transcripts of CPX III in the murine and human brain, but we were not able to detect CPX III mRNA in Northern blots with rat brain mRNA. This indicates that the mCPX III gene is either expressed at very low levels or in a small population of cells in the brain, or for only a brief period of time during brain development. To distinguish between these possibilities, we performed in situ hybridization experiments on mouse brain sections using radiolabeled antisense oligonucleotides as probes. As expected from RNA blot data and EST database searches, CPX IV mRNA was not detectable on brain sections (unpublished data). In contrast, CPX III mRNA was found in many regions of the brain (Fig. 2 B). Most importantly, pyramidal cells in the CA regions of the

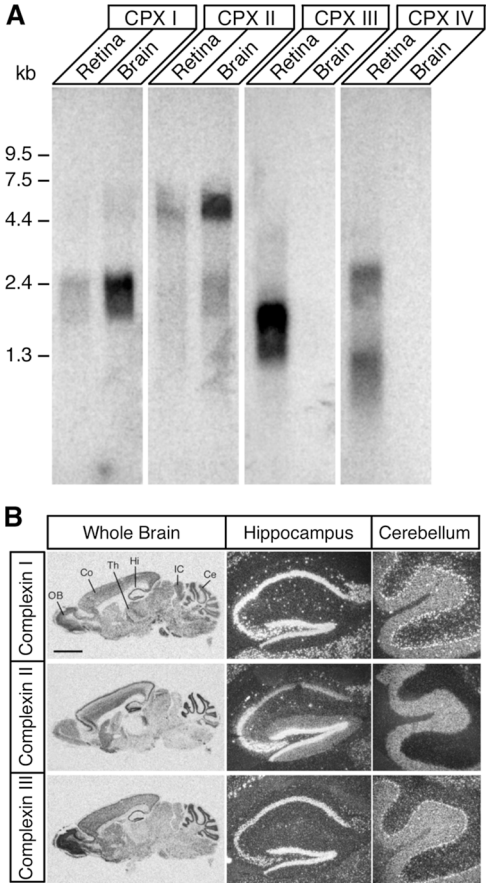

Figure 2. **CPX mRNA expression in brain and retina.** (A) Blots containing poly(A)$^+$-RNA from rat brain and retina, hybridized at high stringency with uniformly labeled full-length cDNA probes for rCPXs I or II, or mCPXs III or IV, and exposed to film for 20 h. (B) Negative X-ray film images showing the distribution of CPXs I, II, and III in adult mouse brain (left), and high magnification bright field images of emulsion dipped slices where silver grains (bright areas) represent the distribution of CPXs I, II, and III in adult mouse hippocampus (middle) and cerebellum (right). Ce, cerebellum; Co, cortex; Hi, hippocampus; IC, inferior colliculus; OB, olfactory bulb; Th, thalamus. Bar: (left) 2 mm and (middle and right) 0.25 mm.

hippocampus as well as granule cells in the dentate gyrus express CPX III mRNA, as well as CPXs I and II mRNAs. In cerebellum, CPX I, II, and III mRNAs were detected in the granule cell layer, and CPXs I and III mRNAs were found in the Purkinje cell layer.

Expression pattern of CPX proteins

For the detection of CPXs III and IV proteins, we generated polyclonal antisera to the human and mouse isoforms using recombinant His_6-tagged full-length proteins as antigens. The antisera showed only very weak cross reactivity with the respective homologous isoform (i.e., CPX III vs. CPX IV), as determined by Western blots of HEK293 cells overexpressing EGFP-tagged full-length mouse CPXs. No cross reactivity of either antiserum with CPX I or CPX II was observed (Fig. S1, available at http://www.jcb.org/cgi/content/full/jcb.200502115/DC1). The antisera raised against the human proteins cross reacted with the respective mouse and rat CPXs III and IV (Fig. 3). The weak cross reactivity of our antisera to CPX III (vs. CPX

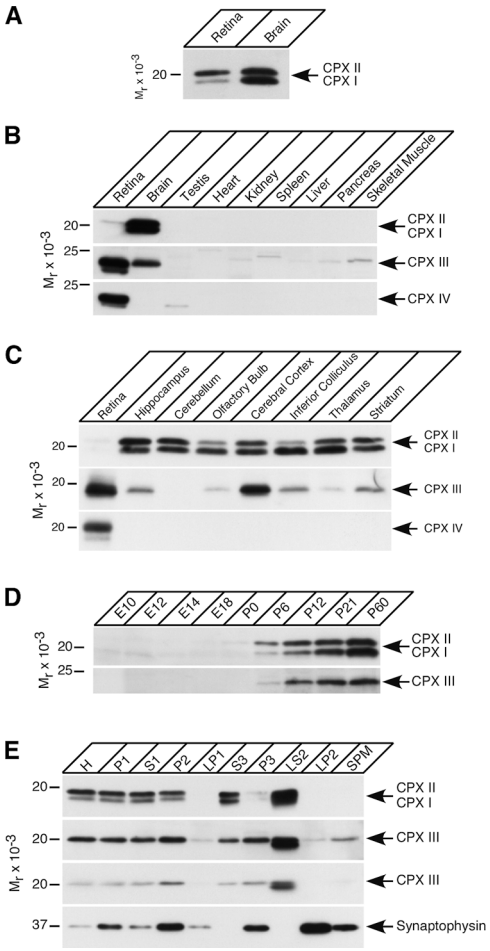

Figure 3. **CPX protein expression in different tissues, brain regions, developmental stages, and brain subcellular fractions.** Homogenates from the indicated rat organs (A and B), rat brain regions (C), brains from mice of different ages (D), and rat cortex subcellular fractions (E) were analyzed by Western blotting using specific antibodies to the indicated proteins (arrows). The two CPX III panels in E show a short (bottom) and long (top) exposure of the same blot. Developmental stages were designated as follows: E, embryonic day; P, postnatal day. Subcellular fractions were designated as described in Materials and methods.

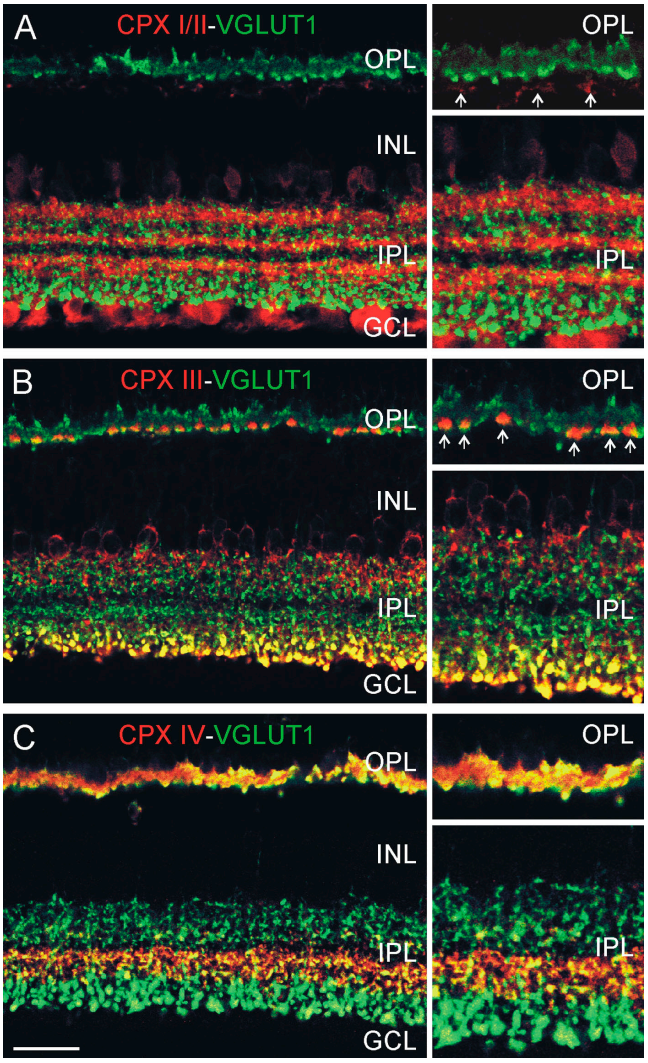

Figure 4. **Differential distribution of CPXs I/II, III, and IV in the mouse retina.** (A–C) Confocal micrographs of vertical sections through mouse retina double labeled for the different CPXs (red) and VGLUT1 (green), as a marker for the glutamatergic synaptic terminals of photoreceptors and bipolar cells. The micrographs to the right show high power views of areas of the OPL and the IPL. (A) Somata of amacrine cells in the INL and of amacrine and ganglion cells in the GCL show CPX I/II immunoreactivity. The processes of CPX I/II labeled amacrine cells stratify in three bands in the IPL. In the OPL, horizontal cell processes are weakly CPX I/II immunoreactive (arrows). There is no colocalization of CPX I/II and VGLUT1. (B) Somata of amacrine cells in the INL and their processes stratifying in a broad band in the IPL, abutting the INL, are labeled for CPX III. The large CPX III immunoreactive structures in the IPL, close to the GCL, and in the OPL, are bipolar and cone photoreceptor terminals (arrows), respectively, as seen in the double labeling with VGLUT1. (C) CPX IV and VGLUT1 colocalize in the IPL and the OPL, indicating the expression of CPX IV in bipolar and photoreceptor cell terminals. OPL, outer plexiform layer (synaptic); INL, inner nuclear layer; IPL, inner plexiform layer (synaptic); GCL, ganglion cell layer. Bar, 20 μm.

IV) and CPX IV (vs. CPX III) that was observed in Western blot experiments (Fig. S1) does not interfere with their ability to selectively label their respective antigens in immunocytochemical experiments in retina. The two antisera produce specific and distinct labeling patterns, indicating their CPX isoform specificity (Figs. 4 and 5).

CPXs I and II were found in rat brain and retina, but with higher expression in brain (Fig. 3 A), CPX III was most strongly expressed in rat retina and much less in rat brain (Fig. 3 B), and CPX IV was only detectable in retina (Fig. 3 B). Apart from the retina, CPX III was detected in hippocampus, olfactory bulb, cortex, inferior colliculus, thalamus, and striatum (Fig. 3 C). In Western blots using mouse central nervous system homogenates, we detected CPX III also in the cerebellum (not depicted).

Like CPXs I and II, CPX III protein expression during mouse brain development is first detectable at P6 and increases to reach a plateau at ~20 d after birth when most synapses have been formed (Fig. 3 D). Analysis of rat cortical subcellular fractions showed that CPXs I and II are soluble while CPX III is associated with both, the cytosolic synaptic fraction (LS2) and membranes, where it is enriched in the light membrane pellet (P3) but also detectable in the crude synaptic vesicular fraction (LP2), and in synaptic membranes (LP1 and SPM; Fig. 3 E).

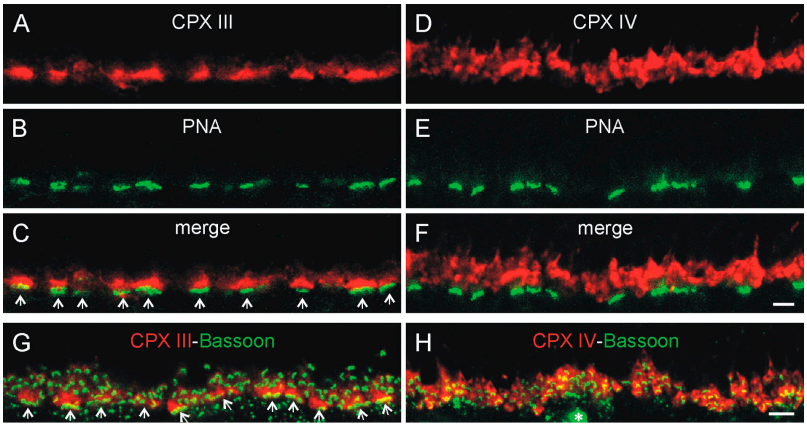

Figure 5. **Differential expression of CPXs III and IV by photoreceptors and their synapses.** (A–C) Confocal micrographs of a vertical section through mouse retina double labeled for CPX III (A, red) and PNA (B, green) as a marker for cone photoreceptor terminals. As seen in the merge of the two stainings, CPX III is strongly expressed in the large cone photoreceptor terminals (C, arrows), and only weakly in the small rod photoreceptor terminals. (D–F) Confocal micrographs of a vertical section through mouse retina double labeled for CPX IV (D, red) and PNA (E, green). The terminals of cone photoreceptors are devoid of CPX IV staining, which is present in the rod photoreceptor terminals (F). (G and H) Confocal micrographs of vertical sections through mouse retina double labeled for CPX III (G, red) and Bassoon (G, green) and for CPX IV (H, red) and Bassoon (H, green). The merge of the stainings confirms the presence of CPX III at cone (G, arrows) and rod ribbon synapses, and of CPX IV at rod ribbon synapses (H). The asterisk in H marks an unspecifically stained blood vessel. Bars, 5 μm.

Distribution of CPXs in the mouse retina

To characterize the cellular and synaptic expression of CPXs in mouse retina, we performed immunocytochemical experiments in which we combined labeling of the different CPXs with markers of individual types of retinal neurons and their synapses.

Initially, we combined each anti-CPX antiserum with an antibody against the vesicular glutamate transporter 1 (VGLUT1; Fig. 4), which specifically marks the glutamatergic synaptic terminals of photoreceptors in the outer plexiform layer (OPL) and of bipolar cells in the inner plexiform layer (IPL) of mouse retina (Johnson et al., 2003; Sherry et al., 2003). The antiserum against CPX I/II (Fig. 4 A) labels somata of amacrine cells in the inner nuclear layer (INL) and somata of displaced amacrine cells and of ganglion cells in the ganglion cell layer (GCL). The CPX I/II-stained processes of amacrine cells stratify in the IPL in three bands of strong fluorescence intensity (Fig. 4 A). The lack of colocalization between CPX I/II and VGLUT1 in the IPL (Fig. 4 A) indicates that CPXs I and II are present at amacrine cell synapses and not at bipolar cell ribbon synapses. Most amacrine cell synapses in the IPL are conventional GABAergic and glycinergic synapses. Double labeling experiments, in which the antisera against CPX I/II were combined with antibodies against GABA or glycine, showed that populations of GABAergic but not glycinergic amacrine cells express CPX I/II (Fig. S2, available at http://www.jcb.org/cgi/content/full/jcb.200502115/DC1). The OPL contains the glutamatergic ribbon synapses of the photoreceptors. Like in the IPL, CPXs I/II do not colocalize with VGLUT1 in the OPL and thus are absent from photoreceptor ribbon synapses (Fig. 4 A). Only the primary processes of horizontal cells are weakly CPX I/II immunoreactive (Fig. 4 A).

CPX III immunoreactivity (Fig. 4 B) is present in both plexiform layers of the retina, the IPL and the OPL. In addition, somata of amacrine cells in the INL are labeled. In the IPL, the broad CPX III immunoreactive band abutting the INL, is formed by processes of amacrine cells, which do not contain VGLUT1 (Fig. 4 B). Double labeling experiments in which the antisera against CPX III were combined with antibodies against GABA or glycine, showed that, unlike CPXs I/II, CPX III is expressed in subpopulations of glycinergic amacrine cells (Fig. S3, available at http://www.jcb.org/cgi/content/full/jcb.200502115/DC1). GABAergic amacrine cells, which are labeled for CPX III, are very rarely found. The second broad immunoreactive band in the IPL, close to the GCL, consists of bipolar cell terminals, which are double labeled for CPX III and VGLUT1 (Fig. 4 B). Double labeling with an antibody against PKCα, identifies these terminals as rod bipolar cell terminals (Fig. S3). In the OPL, the large synaptic terminals of cone photoreceptors are double labeled for VGLUT1 and CPX III (Fig. 4 B).

CPX IV immunoreactivity is present in both synaptic layers of the retina, the IPL and OPL. Here, it colocalizes with VGLUT1 (Fig. 4 C). The distribution of CPX IV immunoreactivity in the two synaptic layers differs from that of CPX III. In the OPL, many smaller photoreceptor terminals are strongly labeled for CPX IV, and in the IPL, putative cone bipolar cell terminals, which are located in a broader band approximately in the middle of the IPL, are CPX IV immunoreactive (Fig. 4 C). CPX IV staining in the IPL does not colocalize with VGLUT3, which has been found in a subset of amacrine cells in mouse retina (Haverkamp and Wassle, 2004; Johnson et al., 2004; not depicted).

These data show that CPXs I/II are expressed at conventional amacrine cell synapses, whereas CPX IV is present at photoreceptor and bipolar cell ribbon synapses. Both types of retinal synapses, ribbon and conventional, contain CPX III.

A comparison of the results of double labeling for CPX III/VGLUT1 and for CPX IV/VGLUT1 indicates that different types of bipolar cells and of photoreceptor cells express the two CPXs (Fig. 4, B and C). To examine this in more detail in photoreceptor cells and their synapses, we performed experiments in which we incubated retinal sections with peanut agglutinin (PNA) together with the antiserum against CPX III (Fig. 5, A–C) or CPX IV (Fig. 5, D–F). The OPL of the retina contains the terminals and synapses of the rod and cone photoreceptors, and PNA specifically marks cone photoreceptor terminals (Blanks and Johnson, 1984). Strong CPX III immunoreactivity is present in the cone photoreceptor terminals, and the rod photoreceptor terminals are only weakly CPX III immunoreactive (Fig. 5, A–C). CPX IV, on the other hand, is strongly expressed in the rod photoreceptor terminals and absent from the cone photoreceptor terminals (Fig. 5, D–F). Costaining of CPXs III

or IV with antibodies to Bassoon, a marker of all photoreceptor ribbon synapses (Brandstätter et al., 1999), also indicates the presence of CPX III at ribbon synapses of cone and rod photoreceptors and of CPX IV at rod photoreceptor ribbon synapses only (Fig. 5, G and H).

Farnesylation of CPXs III and IV

CPXs III and IV carry CAAX-box motifs at their COOH termini (Fig. 1 A) which can be used for stable posttranslational prenylation by addition of either a farnesyl (15-carbon) or a geranylgeranyl (20-carbon) moiety at the cysteine residue, subsequent endoproteolytic cleavage of the AAX tripeptide, and carboxymethylation of the COOH-terminal cysteine residue. The methionine at the last position of the CAAX-box in CPXs III and IV likely causes farnesylation (Zhang and Casey, 1996). To verify that the CAAX-boxes of CPXs III and IV are used for farneslyation in vivo, HEK293 cells were transfected with expression vectors encoding either wild-type (wt) EGFP-CPXs III and IV fusion proteins or mutant EGFP-CPXs III and IV fusion proteins in which the cysteine residues of the CAAX-boxes were replaced by serin residues (C156S in CPX III and C158S in CPX IV). Cells were labeled with the prenyl precursor [^{14}C]mevalonate and harvested, and proteins were solubilized and immunoprecipitated. Samples were analyzed by SDS-PAGE and immunoblotting using an mAb to EGFP, as well as by autoradiography. The immunoblot shows that all proteins were expressed and immunoprecipitated at equal levels (Fig. 6, bottom), but autoradiography of gels showed that only wt proteins were ^{14}C-labeled (Fig. 6, top), indicating that CPXs III and IV are farnesylated in vivo.

Because the posttranslational attachment of prenyl groups is important for targeting proteins to membranes (Zhang and Casey, 1996), we studied the distribution of wt CPXs I, II, III, and IV as well as mutant CPX III-C156S and CPX IV-C158S in HEK293 cells. Initially, we used the EGFP-CPX III and EGFP-CPX IV expression constructs mentioned above, as well as expression constructs encoding full-length CPXs I and II with COOH-terminally fused EGFP. We found that CPXs I, II, and the mutant CPXs III and IV were diffusely distributed in the cytoplasm and the nucleus whereas wt CPXs III and IV were partially plasma membrane associated, present in granular structures in the cytosol, and excluded from the nucleus (Fig. S4 A, available at http://www.jcb.org/cgi/content/full/jcb.200502115/DC1). To circumvent a possible artifact caused by the EGFP-tag we next overexpressed the untagged variants of all CPXs, homogenized the cells, and separated the soluble and membrane-bound pools by centrifugation. Western blot analyses showed that CPXs I and II as well as the main fraction of farnesylation-deficient CPXs III and IV are soluble, whereas wt CPXs III and IV were mainly found in the membranous pellet fraction (Fig. S4 B).

To examine the distribution of the different CPX isoforms in neurons and to test if farnesylation of CPXs III and IV leads to membrane association and affects subcellular localization, primary hippocampal neurons were transfected with the EGFP-tagged CPX constructs described above. Cells were fixed with paraformaldehyde and immunolabeled with an mAb

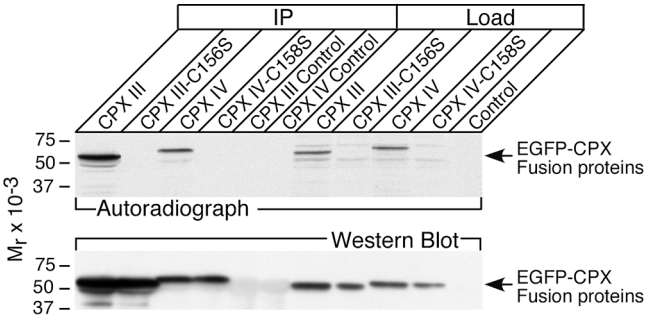

Figure 6. **In vivo farnesylation of CPXs III and IV.** Transfected HEK293 cells coexpressing a mevalonate transporter and either wt EGFP-CPXs III or IV (CPX III, CPX IV), or mutant EGFP-CPXs III or IV (CPX III-C156S, CPX IV-C158S) were labeled with [^{14}C]mevalonate and harvested. Control cells were only transfected with the mevalonate transporter. Whole cell lysates as well as solubilized and immunoprecipitated proteins were analyzed by Western blotting, using an mAb to EGFP (Western blot), and autoradiography (Autoradiograph). The arrows indicate the EGFP-CPX–fusion proteins. All proteins were expressed and precipitated (bottom) but only wt proteins were ^{14}C-labeled (top).

to synaptophysin. In mature cultures analyzed at 14 d in vitro (DIV), CPX I-EGFP and CPX II-EGFP transfected at 4 DIV were distributed diffusely throughout axonal processes and were only weakly enriched in areas that specifically colocalized with the presynaptic marker synaptophysin (Fig. 7). In contrast, EGFP-CPX III and EGFP-CPX IV were enriched in puncta which were characteristic of presynaptic terminals/varicosities and which colocalized with synaptophysin (Fig. 7). Such puncta were not found in processes positive for the dendritic marker MAP2, but were often found along MAP2-positive processes (not depicted), as expected of presynaptic terminals. In contrast, EGFP-CPX III-C156S and EGFP-CPX IV-C158S showed the same diffuse distribution as CPX I-EGFP and CPX II-EGFP (Fig. 7). In immature neurons transfected with constructs expressing EGFP-CPXs III and IV at 8 DIV and immunostained for the trans-Golgi marker TGN38 at 9 DIV, CPXs III and IV were enriched in the trans-Golgi network (unpublished data).

These data indicate that CPXs III and IV are specifically targeted to synaptic terminals in a farnesylation dependent manner. This observation corroborates well with the finding that CPX III is associated with both, the cytosolic synaptic fraction and synaptic membranous compartments in the brain (Fig. 2 E).

SNARE complex binding of novel CPXs

The formation of the synaptic SNARE complex between syntaxin 1 (or syntaxins 2 and 3), SNAP-25, and synaptobrevin/VAMP 2 is a key step in synaptic vesicle exocytosis. CPXs I and II regulate a late step in the transmitter release process (Reim et al., 2001), most likely by binding to the SNARE complex in an antiparallel manner and thereby stabilizing it (Chen et al., 2002). The new CPX isoforms show only limited homology with CPXs I and II (Fig. 1), but most of the conserved residues are found in the core region which forms the SNARE complex binding α-helix (aa 48–70), indicating that the novel CPXs might also act as SNARE complex regulators.

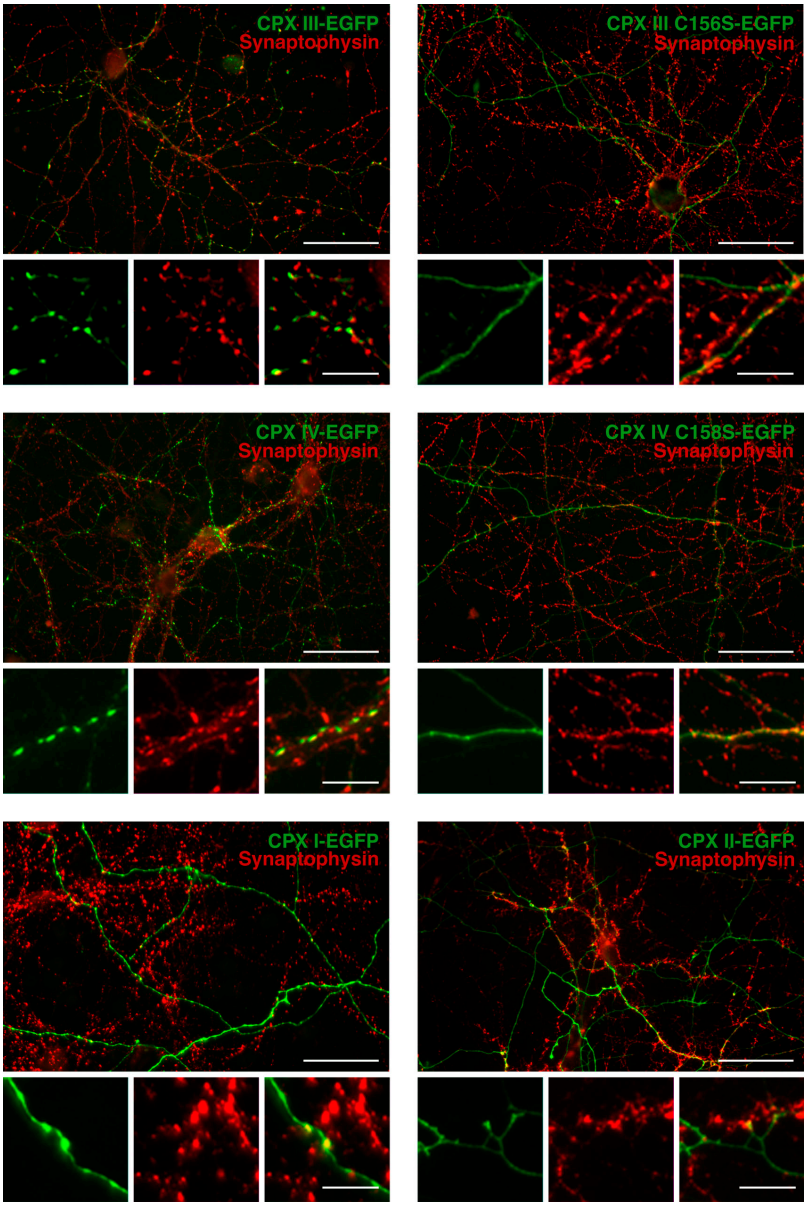

Figure 7. **Distribution of CPXs III and IV in neurons.** Neurons transfected with expression vectors encoding either wt CPX I-EGFP, CPX II-EGFP, EGFP-CPX III, EGFP-CPX IV or farnesylation-deficient EGFP-CPX III-C156S, and EGFP-CPX IV-C158S (all green), and immunostained for synaptophysin (red) to mark presynaptic terminals were analyzed by laser scanning confocal microscopy. Wt CPXs III (top left) and IV (middle left) were concentrated in presynaptic structures of axons and colocalized with synaptophysin, whereas mutant CPXs III (top right) and IV (middle right) as well as wt CPXs I (bottom left) and II (bottom right) showed a diffuse axonal distribution with minor (CPXs I and II) or no (mutant CPXs III and IV) presynaptic accumulation. Bars: (low magnification, large images) 50 μm; (high magnification, small images) 10 μm.

To test whether the new CPX isoforms bind SNARE complexes, cosedimentation assays were performed. GST-fusion constructs encoding full-length rCPX I, mCPX III, and mCPX IV in frame with GST were used for expression of recombinant proteins in bacteria. Initially, recombinant GST-CPX–fusion proteins were incubated with detergent extracts from rat brain synaptosomes, and proteins bound to the GST-CPX beads were analyzed by Western blotting. CPXs I and III bound similar amounts of syntaxin 1, SNAP-25, and synaptobrevin 2 (Fig. 8 A), whereas CPX IV bound the three SNARE components only weakly. Similar results were obtained when we used rat retina extracts as the source of CPX binding proteins (Fig. 8 A). In addition to syntaxin 1, syntaxin 3, which is expressed by retinal photoreceptors and bipolar cells, also bound to CPXs I and III. In a third set of experiments, we used again rat retina extract as protein source but washed with reduced stringency. As expected, we found again significant binding of syntaxins 1 and 3, SNAP-25, and VAMP/synaptobrevin 2 to CPXs I and III, whereas in the CPX IV pellets, only low levels of the SNARE complex components were detected (Fig. 8 A).

These results indicate that all known CPXs interact with SNARE complexes, but CPX IV has a lower SNARE complex binding affinity than all other CPXs.

Function of CPXs III and IV

CPXs III and IV differ from CPXs I and II in structure and expression pattern, but bind SNARE complexes and may therefore still play a role in neurotransmitter release that is equivalent to that of CPXs I and II. To examine this possibility and to test whether farnesylation of the novel CPXs influences their function, we used a knockout (KO) rescue approach. We compared the different CPXs as well as the CPXs III and IV farnesylation mutants with respect to their ability to restore efficient neurotransmitter release in CPX I/II double-deficient (CPX I/II

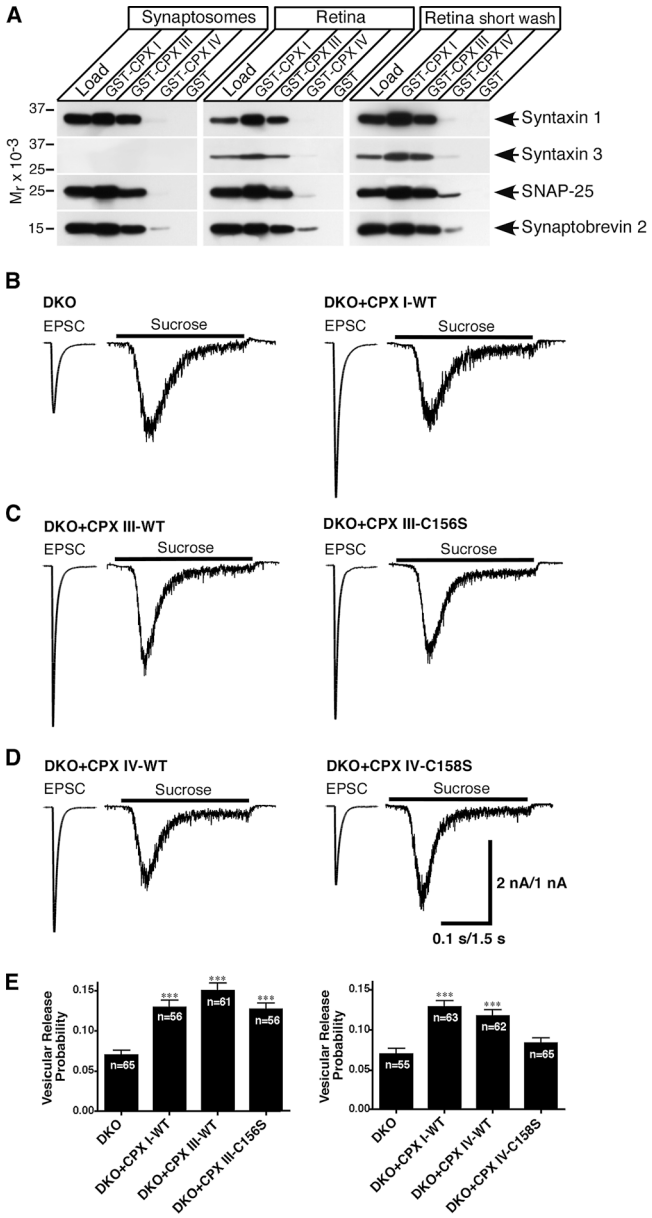

Figure 8. **Characteristics of CPXs III and IV function.** (A) Cosedimentation assays with CPXs I, III, and IV. CPXs I, III, and IV were expressed as GST-fusion proteins, immobilized on glutathione agarose, and incubated with solubilized proteins from crude rat brain synaptosomes or rat retina homogenate. GST-CPX I and GST alone were used as positive and negative controls, respectively. Bound material was analyzed by Western blotting using antibodies to the indicated proteins. Both, CPXs III and IV bind to the SNARE complex, but the necessity to reduce the stringency of the washing steps in order to demonstrate the interaction between the SNARE complex and CPX IV indicates a lower binding affinity. (B–E) Synaptic amplitudes, RRPs and vesicular release probability in glutamatergic CPX I/II DKO neurons and CPX I/II DKO neurons rescued by overexpression of CPXs I, III, or IV. Representative traces showing autaptic EPSCs and responses to hypertonic sucrose solution from a CPX I/II DKO neuron (B, left), and CPX I/II DKO neurons rescued with wt CPX I (C, right), wt CPX III (C, left), CPX III-C156S (C, right), wt CPX IV (D, left), or CPX IV-C158S (D; right). Horizontal bar EPSC, 0.1 s; sucrose solution, 1.5 s. Vertical bar EPSC, 2 nA; sucrose solution, 1 nA. (E) Bar diagrams summarizing mean vesicular release probability for CPX I/II DKO neurons and CPX I/II DKO neurons rescued with wt CPX I, wt CPX III, CPX III-C156S, wt CPX IV, or CPX IV-C158S. Asterisks indicate $P < 0.0001$. Error bars indicate SEM.

double KO [DKO]) neurons. Whole-cell patch clamp recordings were performed on single hippocampal neurons cultured on astrocyte microislands. In this preparation, neurons form recurrent 'autaptic' synapses, which allows the simultaneous measurement of various synaptic release modes originating from the same population of synapses. We measured EPSCs evoked by low frequency (0.2 Hz) action potentials and the size of the readily releasable vesicle pool (RRP), as quantified by integrating the transient inward current induced by a 4-s application of external solution containing 500 mM sucrose (Rosenmund and Stevens, 1996). From the EPSC charge and the RRP charge, the vesicular release probability P_{vr} was calculated as an indicator of the efficiency of Ca^{2+}-triggered neurotransmitter release.

We showed previously that CPXs I and II regulate a late step in the release process. In these studies, we found that CPX I/II DKO neurons exhibited a 50% reduction in P_{vr} and a right shift of the apparent Ca^{2+} sensitivity of release, without changes in the RRP (Reim et al., 2001). These defects were fully rescued by Semliki Forest Virus mediated overexpression of wt CPX I (Fig. 8 B). CPX I/II DKO neurons from four cultures showed an average EPSC amplitude of 3.78 ± 0.33 nA ($n = 120$) and an RRP of 0.81 ± 0.06 nC ($n = 120$), compared with 7.30 ± 0.53 nA ($n = 119$, $P < 0.0001$) and 0.69 ± 0.06 nC ($n = 119$, $P = 0.13$) in CPX I/II DKO neurons overexpressing wt CPX I. P_{vr} was then calculated for each neuron. Upon rescue with wt CPX I, the average P_{vr} was increased by ~90% from 0.069 ± 0.005 ($n = 120$) in CPX I/II DKO neurons to 0.129 ± 0.006 ($n = 119$, $P < 0.0001$) in CPX I/II DKO neurons infected with a virus expressing wt CPX I. These results validate the rescue approach in CPX I/II DKO neurons via Semliki Forest Virus mediated CPX overexpression because overexpression of CPX I reconstituted a wt like P_{vr} in CPX I/II DKO neurons.

We next analyzed the ability of CPXs III and IV to rescue the reduced P_{vr} phenotype of CPX I/II DKO neurons. For that purpose, CPX I/II DKO neurons were compared with CPX I/II DKO neurons overexpressing wt CPX III or CPX III-C156S (Fig. 8 C) and wt CPX IV or CPX IV-C158S (Fig. 8 D). In these experiments, CPX I/II DKO neurons overexpressing wt CPX I served as a parallel-positive control. The average P_{vr} values obtained are summarized in Fig. 8 E. Overexpression of wt CPX III ($P_{vr} = 0.150 \pm 0.010$, $n = 61$, $P < 0.0001$ compared with the CPX I/II DKO) and CPX IV ($P_{vr} = 0.117 \pm 0.007$, $n = 62$, $P < 0.0001$ compared with the CPX I/II DKO) fully rescued CPX I/II DKO neurons, demonstrating that CPXs III and IV can act as positive regulators of neurotransmitter release in hippocampal neurons, as do CPXs I and II. Although the farnesylation of CPX III had little impact on its function under conditions of Semliki Forest Virus mediated overexpression (CPX III-C156S: $P_{vr} = 0.126 \pm 0.008$, $n = 56$, $P < 0.0001$ compared with the CPX I/II DKO), farnesylation of CPX IV was essential for its function as CPX IV-C158S showed only weak rescue activity ($P_{vr} = 0.083 \pm 0.007$, $n = 65$, $P = 0.19$ compared with the CPX I/II DKO).

These data show that CPXs III and IV are functionally similar to CPXs I and II, and that farnesylation of CPX IV is important for its function.

Discussion

We characterized two new CPX isoforms, CPXs III and IV, which form a novel mammalian subfamily of the CPX superfamily of SNARE regulators. A protein sequence comparison between CPXs from different species revealed only limited evolutionary conservation restricted to the region responsible for SNARE complex binding (residues 48–70 of CPX I; Fig. 1 A). In this region, residues that based on structural data (Chen et al., 2002) are thought to be essential for the interaction with the SNARE complex, and which we found to be essential for SNARE complex binding in mutagenesis studies (unpublished data), are conserved among isoforms and species (R^{48}, R^{59}, R^{63}, K^{69}, and Y^{70} of CPX I). Outside the SNARE complex binding region, evolutionary conservation is limited to certain species or one of the two CPX subfamilies. The accessory α-helix that flanks the SNARE complex binding region NH_2-terminally (residues 30–47 in CPX I) is conserved among vertebrate CPXs I and II and also insect CPXs I, but not in CPXs I from other species or in the CPX III/IV subfamily. In the latter, it is interrupted by a short, partially conserved sequence stretch. Within the NH_2 termini of CPXs, only one residue (F^3 in CPX I) is conserved among all isoforms and species. In contrast, a cluster of positive residues COOH-terminal of the SNARE binding region is conserved in all members of the CPX I/II subfamily, irrespective of the species, whereas it is absent from the vertebrate CPX III/IV subfamily. The most striking difference between the vertebrate CPX subfamilies is apparent at their COOH terminus where CPXs III and IV carry an extension with a functional CAAX-box farnesylation site that is absent in CPXs I and II. This CAAX-box is not a recent evolutionary acquisition because homologous sequences, in some cases also at the end of COOH-terminal extensions, are present in many invertebrate CPXs (Fig. 1 A). Apart from the CAAX-box, most of the invertebrate CPXs are more similar to CPXs I and II than to CPXs III and IV (Fig. 1 B). These data indicate that the vertebrate CPXs originate from a common ancestor with a COOH-terminal extension and a CAAX-box, both of which were lost in vertebrate members of the CPX I/II subfamily after separation of the CPX I/II and CPX III/IV subfamilies.

Our expression studies in hippocampal neurons demonstrate that farnesylation of CPXs III and IV at the CAAX-motif mediates their specific presynaptic targeting (Fig. 7). Given the evolutionary conservation of CAAX-motifs in CPXs (CAAM in mouse and human CPXs III and IV, CAAS in *Ciona intestinalis*, and CAAQ in *Hirudo medicinalis*, *Drosophila melanogaster*, *Anopheles gambia*, and *Loligo pealeii*, all of which can be farnesylated; Zhang and Casey, 1996; Fig. 1 A), the same is likely to be true for all other CPXs carrying this motif. The underlying mechanism that causes synaptic targeting of prenylated CPXs remains to be elucidated. It is possible that after synthesis, lipidic or proteinaceous interactions at the level of the trans-Golgi network recruit prenylated CPXs into distinct presynapse-bound membrane compartments with characteristic lipid and protein composition.

The main function of CPXs I and II in SNARE mediated synaptic exocytosis is thought to involve stabilization of SNARE complexes in a tight conformation, thus maintaining a highly Ca^{2+} sensitive pool of readily releasable vesicles (Reim et al., 2001; Chen et al., 2002). Our data indicate that the novel CPX isoforms III and IV act as positive regulators of neurotransmitter release, as do CPXs I and II in the central nervous system, because CPXs III and IV bind to SNARE complexes (Fig. 8 A) and their overexpression rescues the reduced P_{vr} phenotype of CPX I/II DKO neurons (Fig. 8, B–E). Interestingly, farnesylation of CPX III has little impact on its function under conditions of Semliki Forest Virus mediated overexpression whereas farnesylation of CPX IV is essential for its rescue function. It is likely that in the autaptic culture, the effect of loss of CPX III farnesylation can be overcome by its high binding affinity to the SNARE complex (Fig. 8 A). However, the binding affinity of CPX IV to the SNARE complex is much lower than that of CPXs I, II, and III (Fig. 8 A). As a consequence, its membrane association by farnesylation is a critical parameter to reach sufficient local CPX IV concentration for functional SNARE complex binding. This is demonstrated by the almost complete lack of rescue activity of the farnesylation-deficient CPX IV-C158S mutant (Fig. 8, B–E), and represents a unique feature of the ribbon synapse specific CPX IV and its role in controlling neurotransmitter release as compared with other CPX family members.

Our data indicate that prenylation and synaptic targeting of CPXs III and IV are of significant functional relevance. This implies that the loss of the CAAX-box motif in CPXs I and II must be compensated during evolution by other changes in CPX I/II protein structure or the regulation of CPX I/II protein expression in the many neurons of the central nervous system that only express CPXs I and II. Indeed, CPXs I and II appear to bind SNARE complexes with higher affinity than CPX IV (Fig. 8 A). Our Northern blot data (Fig. 2 A) as well as the relative frequency of entries in current EST databases indicate that CPXs I and II are expressed at much higher levels in brain than CPX III. Both of these characteristics, i.e., higher expression levels in brain and high SNARE complex affinity, which may be caused by the unique structural features of CPXs I and II (e.g., in the region of the accessory α-helix and the positively charged cluster COOH-terminal to the SNARE binding region), could in principle contribute to a compensation of the disadvantage that is caused by the loss of COOH-terminal farnesylation, consequent lack of synaptic targeting, and free diffusibility in neurons and their synaptic terminals.

COOH-terminal prenylation of CPXs is unlikely to interfere significantly with SNARE complex binding in vivo because CPXs associate with the SNARE complex in an antiparallel fashion (Chen et al., 2002) such that the prenylated COOH terminus lies at the distal tip of the assembled trans SNARE complex and not at the site of vesicle and plasma membrane contact where v- and t-SNARE proteins are inserted into membranes. A systematic mutagenesis study performed in our laboratory indicates that only mutations of conserved CPX I residues in the helical region that contacts the SNARE complex interfere with SNARE complex binding. In contrast, mutations in the NH_2- and COOH-terminal sequences flanking the SNARE binding region do not interfere with SNARE complex

binding of CPX I (unpublished data). Thus, structural changes in sequences outside of the actual SNARE complex binding surface of CPXs do not interfere with SNARE complex binding, and the same would be expected for the COOH-terminal farnesylation. That this is indeed the case is supported by our functional rescue experiments on CPX I/II double-deficient neurons.

Our electrophysiological rescue experiments in neurons show that the novel CPX isoforms act as positive regulators of synaptic exocytosis, as do CPXs I and II, and that farnesylation of CPX IV increases its activity. Thus, in addition to protein expression levels, the efficacy of CPX action is defined by two functional parameters, SNARE complex affinity and local membrane concentration at the site of vesicle fusion, with the latter parameter being positively modulated by COOH-terminal farnesylation. The case of CPX IV exemplifies that these two parameters can influence each other in a compensatory manner as wt CPX IV (low SNARE complex affinity but high local concentration at synaptic membranes due to farnesylation) is functionally equivalent to CPX I (high SNARE complex affinity but no local enrichment due to the lack of farnesylation), whereas the farnesylation-deficient CPX IV-C158S mutant is functionally compromised (low SNARE complex affinity and no local enrichment due to the lack of farnesylation; Fig. 8, B–E). In view of these considerations, CPX III, in which high SNARE complex affinity and COOH-terminal farnesylation are combined, may represent a particularly effective CPX. Thus, in terms of CPX function, ribbon synapses in the retina have all possible advantages, i.e., the high CPXs III and IV expression levels that are otherwise only found for CPXs I and II at conventional synapses of the central nervous system, and the added value of specific synaptic targeting and plasma membrane anchoring.

CPX III is present at ribbon and conventional synapses in the retina, whereas CPX IV seems to be solely expressed at ribbon synapses. The main CPX form at cone ribbon synapses is CPX III, and at rod ribbon synapses CPX IV. Rods and cones exhibit two kinetically distinct phases of release, a slow component, which is similar in both cell types, and a fast component, which is 10 times faster in cones than in rods (Rabl et al., 2005). With CPXs III and IV we have found constituents of the presynaptic exocytotic machinery that are differentially expressed between rod and cone ribbon synapses. It is possible that the high affinity SNARE-binding, farnesylated CPX III isoform is responsible for the very fast release component in cone photoreceptors.

We postulate that CPXs III and IV contribute to the unique efficacy of transmitter release at retinal ribbon synapses. Their expression and localization in retinal ribbon synapses and their structure and targeting to synapses are characteristics of CPXs III and IV that set them apart from the CPXs present in conventional synapses. These features are also likely to convey particularly efficient release properties to the brain synapses that express CPX III.

Materials and methods

Cloning of human and mouse CPXs III and IV cDNAs

Protein profile searches identified two human genes with homology to CPXs I and II in current genomic databases (CELERA database contigs GA_x5YUV32W5LP and GA_x5YUV32VUQQ). The cDNAs of the new human CPXs, which were designated CPX III and CPX IV, were amplified by PCR from human brain QUICK-Clone cDNA (CLONTECH Laboratories, Inc.). PCR products were subcloned into pCRII-TOPO (Invitrogen) and sequenced using the dideoxy chain termination method with dye terminators on a 373 DNA sequencer (Applied Biosystems). Using primers designed on the basis of the human cDNA sequences of CPXs III and IV, the corresponding mouse cDNAs were amplified from mouse brain QUICK-Clone cDNA (CLONTECH Laboratories, Inc.), subcloned and sequenced as described above.

Northern blots

Rat multiple tissue RNA blots (CLONTECH Laboratories, Inc.) were used to analyze the distribution of CPXs III and IV mRNAs. Poly(A)$^+$ RNA from rat brain and retina was isolated using the Oligotex Direct mRNA Midi/Maxi Kit (QIAGEN). 2 μg poly(A)$^+$ RNA from each tissue were separated on a denaturing formaldehyde agarose gel and blotted to nitrocellulose membrane using standard protocols. Membranes were hybridized at high stringency with uniformly labeled probes derived from rCPX I (GenBank/EMBL/DDBJ accession no. U35098), rCPX II (GenBank/EMBL/DDBJ accession no. U35099), mCPX III (GenBank/EMBL/DDBJ accession no. AY264290), and mCPX IV cDNAs (GenBank/EMBL/DDBJ accession no. AY264291) followed by autoradiography.

In situ hybridization

In situ hybridization experiments were performed as described previously (Augustin et al., 1999). Antisense oligonucleotides representing the following sequences were chosen as probes: bp 34–78 of rCPX I cDNA, bp 50–94 of rCPX II cDNA, bp 115–151 of mCPX III cDNA, and bp 238–282 of mCPX IV cDNA. Sections were viewed with an axiophot microscope (objectives: 20× PlanNeofluar 0.5 NA, and 40× PlanNeofluar 0.75 NA; Carl Zeiss MicroImaging, Inc.) and images were captured with a digital camera (Camedia C3030 Zoom; OLYMPUS) using the Camedia Master software.

Generation of antibodies against CPXs III and IV

Polyclonal antisera directed against CPXs III and IV were generated with His-tagged fusion proteins as antigens (Eurogentech). Recombinant full-length His_6-CPXs III and IV fusion proteins were generated by using the expression plasmids pET-28a-mCPX III and pET-28a-mCPX IV (full-length mouse CPXs III and IV, respectively) as well as pET-28a-hCPX III and pET-28a-hCPX IV (full-length human CPXs III and IV, respectively; all in the pET-28a vector; Novagen).

Western blots

SDS-PAGE and immunoblotting were performed using standard procedures. Immunoreactive proteins were visualized with ECL (Amersham Biosciences). The following antibodies were used for Western blots: pAbs to CPX I/II (1:3,000; Synaptic Systems GmbH), polyclonal antisera to mCPX III (1:1,000), mCPX IV (1:1,000), and the mAb to synaptophysin 1 (1:10,000, Cl 7.2; Synaptic Systems GmbH).

Subcellular fractionation

Subcellular fractionations were prepared essentially as described previously (Jones and Matus, 1974). They were designated as follows: H, homogenate; P1, nuclear pellet; S1, supernatant after synaptosome sedimentation; P2, crude synaptosomal pellet; LP1, lysed synaptosomal membranes; S3, cytosolic fraction; P3, light membrane pellet; LS2, cytosolic synaptosomal fraction; LP2, crude synaptic vesicle fraction; and SPM, synaptic plasma membranes.

Retinal tissue preparation and light microscopic immunocytochemistry

Adult mice were anesthetized deeply with halothane and decapitated. The immunocytochemical labeling was performed by indirect fluorescence (Brandstätter et al., 1999). Retinal sections were incubated in the primary antibodies overnight at RT. In addition to the rabbit anti-CPX III (1:10,000) and anti-CPX IV (1:40,000) pAbs produced and characterized in the present study, the following antibodies were used: a rabbit anti-CPX I/II pAb (1:1,000; Synaptic Systems GmbH), a guinea pig anti-VGLUT1 pAb (1:50,000; CHEMICON International, Inc.), a mouse anti-Bassoon mAb (1:2500; StressGen Biotechnologies), a guinea pig anti-GABA pAb (1:500; CHEMICON International, Inc.), a rat anti-glycine pAb (1:1,000; gift of D. Pow, University of Queensland, Brisbane, Australia), and a mouse anti-PKCα mAb (1:200; Biodesign International). The binding sites of the primary antisera were revealed by secondary antisera, goat anti–rabbit, goat anti–guinea pig, goat anti–rat, or goat anti–mouse IgG coupled to

Alexa 594 (red fluorescence) or Alexa 488 (green fluorescence; diluted 1:500; Molecular Probes). In control experiments, either the primary or secondary antiserum was omitted, resulting in a complete loss of specific immunoreactivity. Sections were examined with a confocal laser scanning microscope (Carl Zeiss MicroImaging, Inc.) equipped with an Ar laser and a HeNe laser and a Plan-Neofluar 40×, NA 1.3 oil objective (LSM5 Pascal; Carl Zeiss MicroImaging, Inc.). High resolution scanning was performed with 2,048 × 2,048 pixels. Projections of 3–5 optical slices (z-axis step 0.48 μm) are shown. Images were adjusted for contrast and brightness using Adobe Photoshop 5.5, and figures were arranged using Corel Draw 9. For PNA, cone synaptic terminals were labeled with fluorescein-tagged PNA. The incubation solution was made up of PNA (Vector Laboratories) diluted 1:20 in 3% normal goat serum (wt/vol) and 1% BSA (wt/vol) in PB. The incubation of the retinal sections with PNA was combined with the incubation in the secondary antiserum against CPX III or CPX IV, goat anti–rabbit IgG coupled to Alexa 594 (1:500; Molecular Probes).

Expression of recombinant proteins in HEK293 cells

Mammalian expression vectors encoding full-length wt rCPX I, rCPX II, mCPX III, and mCPX IV with the EGFP sequence attached at their NH_2 (CPXs III and IV) or COOH (CPXs I and II) termini were constructed in pEGFP-C1 and pEGFP-N1 (CLONTECH Laboratories, Inc.), respectively. The mCPX III-C156S and mCPX IV-C158S mutant constructs were generated from the full-length cDNAs using the QuikChange Site-Directed Mutagenesis Kit (Stratagene) and sequenced. HEK293 cells were grown on glass coverslips coated with 0.5% gelatin and transfected with EGFP expression vectors using the SuperFect transfection method (QIAGEN). After incubation for 48 h cells were washed twice with ice-cold PBS, fixed with 4% PFA in PBS for 20 min at RT, mounted with Fluoromount-G and examined by fluorescence microscopy. Digital images were captured with an LSM510 laser scanning microscope (20×/0.50 Plan-Neofluar objective; Carl Zeiss MicroImaging, Inc.) using the LSM510 software. For Western blot analyses the mentioned wt and mutated CPX cDNAs were cloned into the pcDNA3-IRES-EGFP vector and the corresponding proteins were expressed in HEK293 cells. 1 d after transfection, cells were harvested and homogenized in PBS. Soluble and membranous pools were separated by centrifugation (346,000 g_{max} for 15 min).

Metabolic labeling of EGFP-CPX–fusion proteins with [^{14}C]mevalonic acid and immunoprecipitation

Metabolic labeling of EGFP-CPX–fusion proteins with [^{14}C]mevalonic acid in HEK293 cells was performed as described previously (Collins et al., 2000). After labeling, cells were washed with PBS, scraped into solubilization buffer (150 mM NaCl; 10 mM Hepes/KOH, pH 7.4; 1 mM EGTA; 2 mM $MgCl_2$; 1% Triton X-100; 0.2 mM PMSF; 1 μg/ml aprotinin; and 0.5 μg/ml leupeptin) and stirred on ice for 30 min. Insoluble material was removed by centrifugation (346,000 g_{max} for 15 min). 1.5 ml of each supernatant were incubated with 10 μl of hCPX III and hCPX IV antiserum, respectively (2 h at 4°C). After addition of 30 μl bed volume of protein G Sepharose (Amersham Biosciences) and incubation for 2 h at 4°C, the beads were washed four times with solubilization buffer by centrifugation and resuspension, resuspended in SDS-PAGE sample buffer, and analyzed by SDS-PAGE and immunoblotting using an mAb to GFP (1:1,000; Roche).

Expression of recombinant proteins in neurons

Primary cultures of hippocampal neurons were prepared and transfected as described previously (Dresbach et al., 2003). Cells were fixed with 4% PFA (20 min, at 4°C). Antibodies to synaptophysin (Sigma-Aldrich), TGN38 (BD Transduction Laboratories), and MAP2 (Sigma-Aldrich) were applied in blocking solution at 1:100–1:500 dilutions including 10% horse serum, 2% serum albumin, 5% sucrose, and 0.3% Triton X-100. Coverslips were mounted using Mowiol and viewed using an axioplan microscope (Carl Zeiss MicroImaging, Inc.) equipped with a SpotRT cooled CCD camera (Visitron Systems). Objectives were a 20× PlanApo 0.75 NA, a 40× PlanNeofluar 1.30 NA oil and a 63× PlanApo 1.4 NA oil. Analysis of digital images was performed using MetaVue software (Visitron Systems).

Fusion proteins and cosedimentation assays

Recombinant fusion proteins consisting of GST in frame with rCPX I, mCPX III, or mCPX IV were synthesized in *E. coli* using pGEX-KG expression constructs (Guan and Dixon, 1991). Recombinant proteins were purified on glutathione agarose (Sigma-Aldrich) and used, immobilized on the resin, for cosedimentation assays. Crude synaptosomes from rat brain and rat retina homogenates were solubilized at a protein concentration of 2 mg/ml in solubilization buffer (see protocol for metabolic labeling of CPXs above). After stirring on ice for 10 min, insoluble material was removed by centrifugation (10 min at 346,000 g_{max} and 4°C). The equivalent of 3 mg of total protein was then incubated with 50 μg of immobilized GST-fusion protein and 5 mM DTT for 2 h at 4°C. Beads were washed once (short wash) or three times with solubilization buffer containing 5 mM DTT and 0.1% Triton X-100, resuspended in SDS-PAGE sample buffer, and analyzed by SDS-PAGE and immunoblotting. The following antibodies were used for immunodetection: mAbs to syntaxin 1 (1:10,000, Cl 78.2), synaptobrevin 2 (1:10,000; Cl 69.1), and SNAP-25 (1:5,000; Cl 71.1, all purchased from Synaptic Systems GmbH), and a polyclonal antiserum to syntaxin 3 (1:1,000; Morgans et al., 1996).

Culture and electrophysiology of autaptic hippocampal neurons

Primary hippocampal neurons were prepared from newborn CPX I/II DKO mice and grown on astrocyte microislands as described previously (Reim et al., 2001; Rosenmund et al., 2002). For each experiment, approximately equal numbers of neurons from the respective groups were measured on the same DIV (9–14 DIV). Whole-cell patch clamp recordings were performed 9–11 h after Semliki Forest Virus infection (Ashery et al., 2000), as described previously (Rosenmund et al., 2002). Semliki Forest Virus constructs were designed to encode the respective CPX, followed by an IRES and the EGFP cDNA. This allowed us to identify infected cells and to estimate the expression level of the constructs. The cellular EGFP expression levels were similar for all tested construct. Data are presented as mean ± standard error. Statistical significance of differences between two groups was estimated by unpaired nonparametric *t* test.

Online supplemental material

Fig. S1 shows the cross reactivities of antibodies to CPX isoforms using proteins from HEK293 cells transfected with CPX I-EGFP, CPX II-EGFP, EGFP-CPX III, and EGFP-CPX IV. Fig. S2 shows the differential expression of CPX I/II by amacrine cells. Fig. S3 shows the expression of CPX III by amacrine and bipolar cells. Fig. S4 shows the distribution of EGFP-tagged CPX proteins in HEK293 cells. Online supplemental material is available at http://www.jcb.org/cgi/content/full/jcb.200502115/DC1.

We thank T. Hellmann and A. Staab for excellent technical assistance, F. Benseler, S. Handt, and I. Thanhäuser for DNA sequencing and oligonucleotide synthesis, and H. Deng, D. Reuter, and T. Rosenmund for cell culture and virus production.

This work was supported by the Max-Planck-Society, by grants from the Deutsche Forschungsgemeinschaft (SFB523/B9 to N. Brose, SFB269/B4 to J.H. Brandstätter), by the Brown Foundation (to C. Rosenmund), and by an INTAS grant (01-2095 to N. Brose).

Submitted: 18 February 2005
Accepted: 14 April 2005

References

Ashery, U., F. Varoqueaux, T. Voets, A. Betz, P. Thakur, H. Koch, E. Neher, N. Brose, and J. Rettig. 2000. Munc13-1 acts as a priming factor for large dense-core vesicles in bovine chromaffin cells. *EMBO J.* 19:3586–3596.

Augustin, I., A. Betz, C. Herrmann, T. Jo, and N. Brose. 1999. Differential expression of two novel Munc13 proteins in rat brain. *Biochem. J.* 337:363–371.

Blanks, J.C., and L.V. Johnson. 1984. Specific binding of peanut lectin to a class of retinal photoreceptor cells. A species comparison. *Invest. Ophthalmol. Vis. Sci.* 25:546–557.

Brandstätter, J.H., E.L. Fletcher, C.C. Garner, E.D. Gundelfinger, and H. Wässle. 1999. Differential expression of the presynaptic cytomatrix protein Bassoon among ribbon synapses in the mammalian retina. *Eur. J. Neurosci.* 11:3683–3693.

Chen, X., D.R. Tomchick, E. Kovrigin, D. Arac, M. Machius, T.C. Südhof, and J. Rizo. 2002. Three-dimensional structure of the complexin/SNARE complex. *Neuron.* 33:397–409.

Collins, S.P., J.L. Reoma, D.M. Gamm, and M.D. Uhler. 2000. LKB1, a novel serine/threonine protein kinase and potential tumour suppressor, is phosphorylated by cAMP-dependent protein kinase (PKA) and prenylated in vivo. *Biochem. J.* 345:673–680.

Dick, O., S. tom Dieck, W.D. Altrock, J. Ammermüller, R. Weiler, C.C. Garner, E.D. Gundelfinger, and J.H. Brandstätter. 2003. The presynaptic active zone protein Bassoon is essential for photoreceptor ribbon synapse formation in the retina. *Neuron.* 37:775–786.

Dresbach, T., A. Hempelmann, C. Spilker, S. tom Dieck, W.D. Altrock, W. Zuschratter, C.C. Garner, and E.D. Gundelfinger. 2003. Functional regions of the presynaptic cytomatrix protein Bassoon: significance for synaptic

targeting and cytomatrix anchoring. *Mol. Cell. Neurosci.* 23:279–291.

Guan, K.L., and J.E. Dixon. 1991. Eukaryotic proteins expressed in *Escherichia coli*: an improved thrombin cleavage and purification procedure of fusion proteins with glutathione S-transferase. *Anal. Biochem.* 192:262–267.

Haverkamp, S., and H. Wassle. 2004. Characterization of an amacrine cell type of the mammalian retina immunoreactive for vesicular glutamate transporter 3. *J. Comp. Neurol.* 468:251–263.

Heidelberger, R., and G. Matthews. 1992. Calcium influx and calcium current in single synaptic terminals of goldfish retinal bipolar neurons. *J. Physiol.* 447:235–256.

Heidelberger, R., C. Heinemann, E. Neher, and G. Matthews. 1994. Calcium dependence of the rate of exocytosis in a synaptic terminal. *Nature.* 371:513–515.

Jahn, R., T. Lang, and T.C. Südhof. 2003. Membrane fusion. *Cell.* 112:519–533.

Johnson, J., N. Tian, M.S. Caywood, R.J. Reimer, R.H. Edwards, and D.R. Copenhagen. 2003. Vesicular neurotransmitter transporter expression in developing postnatal rodent retina: GABA and glycine precede glutamate. *J. Neurosci.* 23:518–529.

Johnson, J., D.M. Sherry, X. Liu, R.T. Fremeau Jr., R.P. Seal, R.H. Edwards, and D.R. Copenhagen. 2004. Vesicular glutamate transporter 3 expression identifies glutamatergic amacrine cells in the rodent retina. *J. Comp. Neurol.* 477:386–398.

Jones, D.H., and A.I. Matus. 1974. Isolation of synaptic plasma membrane from brain by combined flotation-sedimentation density gradient centrifugation. *Biochim. Biophys. Acta.* 356:276–287.

Mandell, J.W., E. Townes-Anderson, A.J. Czernik, R. Cameron, P. Greengard, and P. De Camilli. 1990. Synapsins in the vertebrate retina: absence from ribbon synapses and heterogenous distribution among conventional synapses. *Neuron.* 5:19–33.

Morgans, C.W. 2001. Localization of the alpha (1F) calcium channel subunit in the rat retina. *Invest. Ophthalmol. Vis. Sci.* 42:2414–2418.

Morgans, C.W., J.H. Brandstätter, J. Kellermann, H. Betz, and H. Wässle. 1996. A SNARE complex containing syntaxin 3 is present in ribbon synapses of the retina. *J. Neurosci.* 16:6713–6721.

Nachman-Clewner, M., R. St. Jules, and E. Townes-Anderson. 1999. L-type calcium channels in the photoreceptor ribbon synapse: localization and role in plasticity. *J. Comp. Neurol.* 415:1–16.

Parsons, T.D., and P. Sterling. 2003. Synaptic ribbon. Conveyor belt or safety belt? *Neuron.* 37:379–382.

Parsons, T.D., D. Lenzi, W. Almers, and W.M. Roberts. 1994. Calcium-triggered exocytosis and endocytosis in an isolated presynaptic cell: capacitance measurements in saccular hair cells. *Neuron.* 13:875–883.

Rabl, K., L. Cadetti, and W.B. Thoreson. 2005. Kinetics of exocytosis is faster in cones than in rods. *J. Neurosci.* 25:4633–4640.

Reim, K., M. Mansour, F. Varoqueaux, H.T. McMahon, T.C. Südhof, N. Brose, and C. Rosenmund. 2001. Complexins regulate a late step in Ca^{2+}-dependent neurotransmitter release. *Cell.* 104:71–81.

Rieke, F., and E.A. Schwartz. 1996. Asynchronous transmitter release: control of exocytosis and endocytosis at the salamander rod synapse. *J. Physiol.* 493:1–8.

Rosenmund, C., and C.F. Stevens. 1996. Definition of the readily releasable pool of vesicles at hippocampal synapses. *Neuron.* 16:1197–1207.

Rosenmund, C., A. Sigler, I. Augustin, K. Reim, N. Brose, and J.S. Rhee. 2002. Differential control of vesicle priming and short-term plasticity by Munc13 isoforms. *Neuron.* 33:411–424.

Schmitz, F., A. Königstorfer, and T.C. Südhof. 2000. RIBEYE, a component of synaptic ribbons: a protein's journey through evolution provides insight into synaptic ribbon function. *Neuron.* 28:857–872.

Sherry, D.M., M.M. Wang, J. Bates, and L.J. Frishman. 2003. Expression of vesicular transporter 1 in the mouse retina reveals temporal ordering in development of rod vs. cone and ON vs. OFF circuits. *J. Comp. Neurol.* 465:480–498.

Stevens, C.F., and T. Tsujimoto. 1995. Estimates for the pool size of releasable quanta at a single central synapse and for the time required to refill the pool. *Proc. Natl. Acad. Sci. USA.* 92:846–849.

von Gersdorff, H., E. Vardi, G. Matthews, and P. Sterling. 1996. Evidence that vesicles on the synaptic ribbon of retinal bipolar neurons can be rapidly released. *Neuron.* 16:1221–1227.

Zhang, F.J., and P.J. Casey. 1996. Protein prenylation: molecular mechanisms and functional consequences. *Annu. Rev. Biochem.* 65:241–269.